ELSEVIER

Thermochimica Acta 387 (2002) 29–38

thermochimica acta

www.elsevier.com/locate/tca

HT-XRD, IR and Raman characterization studies of metastable phases emerging in the thermal genesis course of monoclinic zirconia via amorphous zirconium hydroxide: impacts of sulfate and phosphate additives

A.A.M. Ali, M.I. Zaki*

Chemistry Department, Faculty of Science, Kuwait University, P.O. Box 5969, Safat 13060, Kuwait

Received 21 May 2001; received in revised form 15 September 2001; accepted 25 September 2001

Abstract

High-temperature X-ray powder diffractometry was performed on pure and impregnated (with sulfate and phosphate additives) $Zr(OH)_4$ while being in situ heated (in air) to different temperatures up to 1000 °C. Accordingly, portions of these materials were ex situ calcined at some selected temperatures within the temperature regime examined. The calcination products were subjected to Fourier-transform laser Raman and infrared spectroscopic analyses. The results showed the pure hydroxide to decompose into low-temperature stable monoclinic zirconia (m-ZrO_2) in a slow process intermediated by metastable tetragonal (t-ZrO_2) and/or cubic (c-ZrO_2) phases. The metastability of the intermediate phases was, therefore, considered to be a consequence of the slow kinetics of conversion. Moreover, high surface energy (small particle size) of these phases was suggested as an additional reason for their existence, in terms of consistent literature data. The sulfate and, particularly, phosphate additives were shown to slow further the formation of m-ZrO_2. This has been suggested to arise from (i) suppression of particle sintering (growth), and (ii) phosphate stabilization (most likely) of c-ZrO_2. Results of the present investigation may help a better understanding of phase transitions occurring during the thermal genesis of zirconia-based solid acids from an amorphous parent material, a domain that has hitherto received little agreement in the literature.

Keywords: Zirconia; Sulfated zirconia; Phosphated zirconia; Polymorphism; High-temperature X-ray diffractometry; Raman spectroscopy; Infrared spectroscopy

1. Introduction

Zirconia (ZrO_2) is an interesting catalytic material that may exist in three different, true polymorphs under atmospheric pressure [1,2]: monoclinic (m-ZrO_2) at $\leq$750 °C, tetragonal (t-ZrO_2) at 1200–2000 °C, and cubic (c-ZrO_2) zirconia at $\geq$2100 °C. Each of these polymorphs may, however, exist in either of the following states: metastable (often sustained by the co-existence of a true phase), stabilized (by foreign agents) and strained (due to high temperature, or while being transformed) state [2]. Probably the prominent application of zirconia in catalysis is as a support material for metal, metal oxide and acid catalysts. When supported on zirconia, (i) copper is a superior methanol synthesis catalyst [3], Rh is a stronger CO hydrogenation catalyst

* Corresponding author. Fax: +965-4846946.
E-mail address: zaki@mail.kuniv.edu.kw (M.I. Zaki).

0040-6031/02/$ – see front matter
PII: S0040-6031(01)00824-3

[4], Ni is a much more selective [5] and sulfur-tolerant [6] methanation catalyst, and sulfate and phosphate radicals are more active and selective skeletal isomerization acid catalysts, than when supported on traditional oxide supports (e.g. alumina, silica, etc.). The most prominent of these, however, is its application in acid catalysis. As a matter of fact, the greatest share of the large amount of research dedicated for preparing and characterizing catalytic solid acids and superacids has been encoded zirconia-based materials (SO_4^{2-}/ZrO_2, PO_4^{3-}/ZrO_2 and ZrP_2O_7) [7–10]. This laboratory has joined the forces with the international endeavor, and contributed three such studies [11–13].

The large body of accumulated characterization results on zirconia-based solid acids, which has been obtained employing a wide range of surface and bulk analytical techniques, have revealed areas of agreement, as well as disagreement, between researchers in the field. For instance, it is largely agreed that (i) sulfated and phosphated zirconia catalysts are produced by calcination at 550–650 °C of *m*-ZrO_2, or amorphous $Zr(OH)_4$, impregnated with ammonium sulfate or phosphate compounds [8,14], (ii) sulfate additives are capable of generating on zirconia derived from *m*-ZrO_2, or amorphous $Zr(OH)_4$, BrØnsted acid sites (surface-$O_3SOH^{\delta+}$), and promoting the acidity of weak Lewis sites (Zr^{4+}) via its known electron withdrawing power [14], and (iii) phosphate additives are likewise, however, only when $Zr(OH)_4$ is the parent material employed [8,11–18]. Infrared and Raman spectroscopic analyses [13], as well as others' conclusions [17,19], have facilitated attributing the unique behavior of the phosphate to the formation of zirconium pyrophosphate (ZrP_2O_7-like) species.

Formation of pyrophosphate species has been proposed [13] to help stabilize *c*-ZrO_2 as a minor phase in the catalyst composition; the major phase being *m*-ZrO_2. Despite the lack of sufficient experimental evidence, this presumption has been considered [13] plausible in terms of two arguments. The first is that crystalline ZrP_2O_7 assumes similarly a cubic structure [20]. The second argument is that thermal decomposition of the parent hydroxide ($Zr(OH)_4$), to give phosphated ZrO_2, facilitates occurrence of solid–solid PO_4^{3-}/ZrO_2 at the immediate vicinity of the thermal genesis of the oxide, which is a requirement if the phosphate were to influence the crystallization into *c*-ZrO_2. A similar envisagement has also been conceived for the stabilization of *c*-ZrO_2 under the influence of some cationic additives (viz. Ce^{4+}, Y^{3+}, Ca^{2+} and Mg^{2+}) in a ceramic preparation course [21–23]. Formation of phosphate-stabilized *c*-ZrO_2 is, however, a point of disagreement amongst researchers. We quote, as for example, the recent X-ray diffraction (XRD) results of Mekhemer and Ismail [10], which led them to confine the phosphate stabilizing function to *t*- rather than *c*-ZrO_2 phase. It is worth noting, that we could not exclude this possibility in earlier XRD studies [12,13], due to the lack of XRD resolution dealing with such largely isomorphous (short-range) structures [1,24]. Another point of continuous debate is the mode of anchorage of sulfate (and phosphate) species onto the surface of the final catalyst [17,25–27], viz. whether monomeric, bridging, multi-centered, or chelating.

The present investigation was undertaken to shed more light on the nature of sulfate- and phosphate-stabilized zirconia phases in the course of thermal genesis of sulfated and phosphated zirconia solid acids from corresponding $Zr(OH)_4$-based precursors. This was stimulated by (i) the existing disagreement in the literature over this issue; (ii) availability of the potential of high-temperature X-ray powder diffractometry (HT-XRD) to examine zirconia polymorphic transitions during in situ heating-cooling treatments at 25–1000 °C; (iii) recent literature data [28,29] revealing dependence of CO_2 methanation activity of Ni/ZrO_2 catalyst on the phase composition of the zirconia support; and (iv) literature data [1,30–32] relating formation of metastable *t*- or *c*-ZrO_2 to utilization of amorphous zirconia parent materials (such as the present $Zr(OH)_4$), and attributing their existence to thermodynamic, kinetic and structural reasons [30–32]. Specifically speaking, Lajavardi et al. [32], in a very recent series of rigorous HT-XRD and Raman studies, have found *c*-ZrO_2 to form first, and, then, progressively transform to *t*- and *m*-ZrO_2, depending primarily on the particle size (i.e. the surface energy and presence of impurities at grain boundaries). Laser Raman (LRa) and infrared (IR) spectroscopies were applied in the present investigation to examine calcination products at some selected temperatures, so as to compensate for XRD shortcomings dealing with isomorphous short-range structures [1,24].

2. Experimental

2.1. Materials

The $Zr(OH)_4$ (denoted ZrOH) was a MEL (Manchester, UK) product no. XZO631/01. It was found previously [13] to have the molecular formula of $Zr(OH)_4 \cdot H_2O$, and that the excess mole of water could be eliminated by drying in air at 80 °C for 24 h. Therefore, impregnated ZrOH materials (viz. $(NH_4)_2SO_4$/ZrOH and $(NH_4)_2HPO_4$/ZrOH) were obtained as detailed previously [13], by stirring a 6.5 g portion of the dried hydroxide in a 75 ml portion of aqueous solutions of the sulfate or phosphate salt (Chemtel AR-grade products, UK) at room temperature (RT) for 30 min. Slurries, thus, obtained were dried at 80 °C for 48 h and the resulting materials are denoted below as SZrOH and PZrOH, respectively. Then, they were ex situ calcined at some selected temperatures in the range 400–1000 °C for 3 h. The calcination temperatures were chosen on the basis of high-temperature X-ray diffractometry results (vide infra), and the products are discerned below by an Arabic numeral symbolizing the calcination temperature applied. Hence, SZrOH4 means the 400 °C calcination product of the sulfate-impregnated hydroxide, whereas PZrOH6 designates the 600 °C calcination product of the phosphate-impregnated hydroxide. Based on the concentration of the impregnating solution, the calcination products should contain ≈5 wt.% SO_4^{2-} or PO_4^{3-} species.

For control purposes, a dried portion of the original hydroxide was similarly wet-treated, dried (denoted ZrOH) and ex situ calcined, but in the absence of the sulfate and phosphate compounds. Temperature-symbolizing numerals similarly indicate the calcination products.

2.2. High-temperature X-ray powder diffractometry (HT-XRD)

The HT-XRD was carried out (at $10 < 2\theta < 80^\circ$) on uncalcined test samples (ZrOH, SZrOH and PZrOH), applying an in situ temperature-programmed heating mode, using a Siemens D5000 diffractometer equipped with Ni-filtered CuKα radiation ($\lambda = 1.5406$ Å). The diffractomer was operated with 1° diverging and receiving slits at 50 kV and 40 mA, and a continuous scan was carried out with a step size of 0.04° and a step time of 15.0 s. The sample temperature was increased in air (at 20 °C/min) from RT up to a given HT in the range 100–1000 °C; then, the temperature was leveled off directly to RT. For instance, in the range RT–400 °C, (i) a diffractogram (designated RT(I)) was taken of the test sample at room temperature, (ii) sample temperature was increased to 100 °C, maintained for 10 min, and a diffractogram (designated 100 °C) was measured of the sample, and (iii) sample temperature was, then, brought up to 200 °C, maintained for 10 min, and a diffractogram (designated 200 °C) was taken of the sample. Step (iii) was repeated to measure diffractograms at 300 and 400 °C. Subsequently, the 400 °C heated material was allowed to cool directly to RT, maintained at RT for 1 or 24 h, and a diffractogram (designated RT (1 h) or RT (24 h)) was measured. This latter RT-cooled material (namely for 1 h) was the test sample for the subsequent RT–HT′ loop (where HT′ > HT), and so on. An on-line automatic search system (PDF Data Base) facilitated the observed data match with JCPDS-ICDD standards, and hence, crystalline phase identification.

2.3. Vibrational spectroscopy

Ex situ calcination products of ZrOH, SZrOH and PZrOH were subjected to Fourier-transform Laser Raman (LRa) and infrared (IR) spectroscopic analyses. LRa spectra were taken using lightly compacted test samples, at 200–3600 cm^{-1} and a resolution of 0.2 cm^{-1}, using a Perkin-Elmer System 2000 Raman spectrometer (USA) equipped with a near infrared diode pumped Nd:YAG laser (1.064 μm). The laser power at the sample was in the range of 50–100 mW. On the other hand, IR transmission spectra were taken using thin wafers of KBr-supported test samples (<1 wt.%) at 400–4000 cm^{-1} and a resolution of 5.3 cm^{-1}, using a Bruker IFS-25 spectrophotometer.

3. Results and discussion

3.1. X-ray powder diffractograms

ZrOH. Fig. 1 displays HT-XRD diffractograms obtained for pure ZrOH at different temperatures on

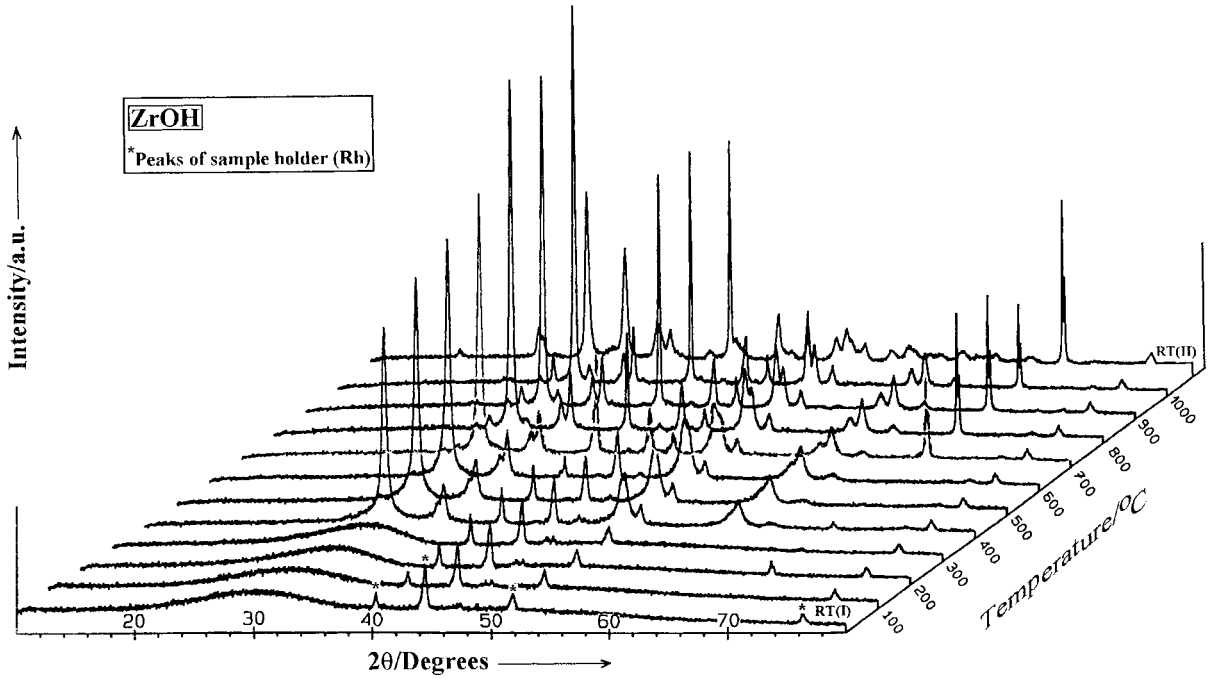

Fig. 1. High-temperature X-ray powder diffractograms obtained following in situ heating in air of pure zirconium hydroxide (ZrOH) at the temperatures indicated for 10 min. RT(II) marks the diffractogram exhibited by the 1000 °C heated sample after cooling at RT for 24 h.

heating from room temperature (RT(I)) up to 1000 °C. The diffractogram obtained after subsequent cooling to room temperature (RT(II)) is also displayed. Excluding the four ∗-labeled peaks of the sample holder (Rh), it is obvious that the hydroxide remains amorphous on heating up to 300 °C. The corresponding diffractograms show nothing, but a broad hump centered around 2θ of 30°. A similar hump was observed previously [30] for amorphous zirconium hydroxide, and has been considered indicative of short-range structures isomorphous to t-ZrO_2 with atoms being arranged for incipient crystallization to the tetragonal structure. Those authors [30] have based their consideration on the close similarity between the 2θ value of the hump (∼30°) and that at which the strongest peak of t-ZrO_2 occurs ($2\theta = 30.17°$, JCPDS #17–923). However, the same could also be applicable to the strongest peak of c-ZrO_2 (30.48°, JCPDS #27–997). Fig. 1 also shows that it was not until the temperature reached 400 °C that an XRD pattern of the test material was observed. This result is in line with earlier thermal analysis results [13] showing amorphous $Zr(OH)_4$ to lose weight gradually on heating up to 400 °C, corresponding to dehydration into ZrO_2. The product was found to suffer a weight-invariant, exothermic event (glow phenomenon) near 440 °C marking the onset of crystallization process. The diffraction peaks monitored are rather broad, thus, indicating a small particle size. Insertion of peak width at half maximum (in radians unit) in Scherrer equation [33] resulted in an average particle size of 160 ± 20 Å. It is reasonably close to what has recently been reported [32] for the first emerging crystalline product of decomposition of zirconium hydroxide (50–140 Å).

Moreover, Fig. 1 helps making the following general observations: (i) peaks of the diffraction pattern exhibited at 400 °C are rendered stronger, but not significantly narrower, upon further heating up to 700 °C, (ii) a new diffraction pattern emerged at 800 °C; its peaks are narrower (average particle size ∼220 ± Å) and grew stronger upon further heating up to 1000 °C, at the expense of peaks of the low-temperature pattern, and (iii) peaks of the high-temperature pattern (at 1000 °C) predominated following subsequent cooling to room temperature (RT(II)). Hence, HT-XRD results (Fig. 1) reveal that non-isothermal heating of

amorphous ZrOH leads to formation of a low-temperature crystalline zirconia at 400–600 °C that undergoes a transition at 800 °C into high-temperature zirconia assuming a different crystalline structure. The fact that this latter zirconia phase developed only gradually with heating up to 1000 °C, but considerably upon a subsequent cooling to RT may imply that low-temperature zirconia is metastable, whereas the high-temperature zirconia is the low-temperature stable phase (i.e. a true phase).

To facilitate a rigorous inspection of the HT-XRD results of ZrOH, peaks displayed over the indicative range ($2\theta = 27$–32°) of the diffractograms are compared to those monitored over the same range, but after cooling to RT, in Fig. 2. The single peak observed at 400 °C must characterize the low-temperature zirconia phase. The corresponding d-spacing (2.946 Å) lies

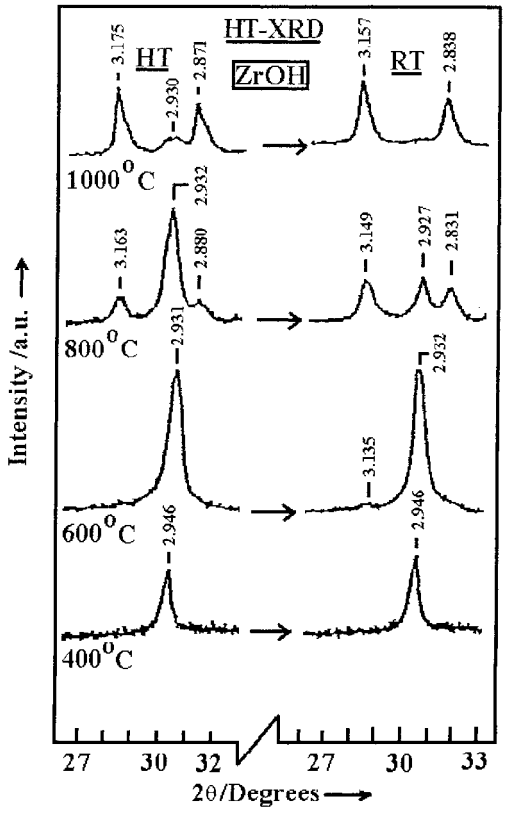

Fig. 2. X-ray powder diffractograms obtained following in situ heating of ZrOH at the temperatures indicated for 10 min (HT-entitled) and subsequent cooling at room temperature (RT-entitled) for 24 h.

intermediate between the d-spacing values at which the strongest ($I/I_o = 100\%$) diffraction peaks of *c*-(2.96 Å) and *t*-ZrO_2 (2.93 Å) are observed (JCPDS #27–997 and #17–923, respectively). Thus, heating of ZrOH to 400 °C results in the formation of *t*- and/or *c*-ZrO_2. The diffraction peak is shown to persist to subsequent cooling to RT.

At 600 °C, the diffraction peak is maintained, whereas the corresponding d-spacing is shifted towards a value (2.931 Å) accounting for *t*-rich ZrO_2. The subsequent cooling to RT is shown to result in the emergence of a very weak diffraction feature at the higher d-spacing side (>2.932 Å) of the peak (namely at 3.135 Å). At 800 °C, this weak feature grew stronger and a companion weak feature emerged at the lower d-spacing side (<2.932 Å) of the major peak (namely at 2.880 Å). These 2-weak diffraction peaks assume d-spacings very close to those (3.16 and 2.87 Å) of the two strongest peaks ($I/I_o = 100$ and 70%, respectively) of *m*-ZrO_2 (cf. JCPDS #37–1484). Increasing the temperature to 1000 °C, is shown (Fig. 2) to develop the peaks assignable to *m*-ZrO_2 at the expense of the peak (at 2.930 Å) due to *t*-rich ZrO_2. This process is shown to be enhanced on subsequent cooling to RT. Consequently, zirconia is almost completely transformed into the monoclinic structure.

Hence, the above results show the metastable, low-temperature zirconia to be *c*-rich at the immediate vicinity of its formation (i.e. at 400 °C), which is, then, transformed into *t*-rich zirconia at $\geq$600 °C. On the other hand, the high-temperature zirconia, which is definitely the stable phase at low temperatures, is *m*-ZrO_2. The accompanying change in peak width was found to reaveal a particle growth from an average size of ~160 to 240 ± 20 Å as *m*-ZrO_2 forms. This indicates that the average particle size of *m*-ZrO_2 is larger than that of metastable zirconia (*t*- and/or *c*-ZrO_2).

A number of recent studies [30,32] have attributed the existence of metastabe zirconia in the low temperature regime to its higher surface energy (smaller particle size) than *m*-ZrO_2, as well as to the slow kinetics of its transformation into the latter phase. In a series of isothermal HT-XRD studies, Lajavardi et al. [32] have suggested *c*-ZrO_2 to crystallize first from an amorphous parent, and, then, progressively transform into *t*- and *m*-ZrO_2 at temperatures as low as 320–400 °C. These authors [32] have concluded that the cubic, tetragonal and monoclinic phases of zirconia

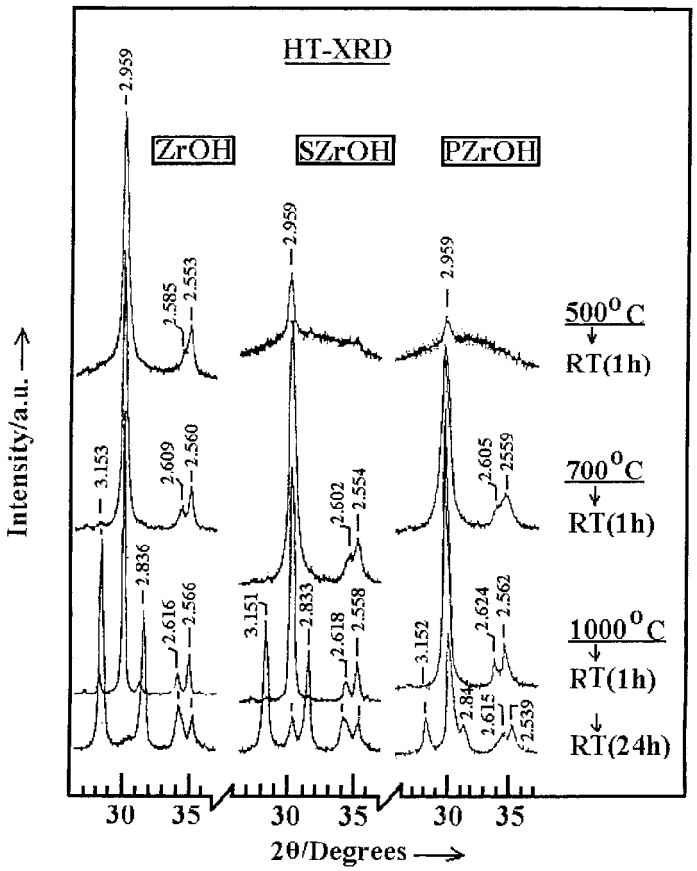

Fig. 3. Room-temperature X-ray powder diffractograms obtained following cooling at RT (for periods indicated) of in situ preheated samples of pure (ZrOH), and sulfate- (SZrOH) and phosphate-impregnated (PZrOH) zirconium hydroxide at the temperatures indicated (for 10 min).

are distinct functions of crystallite size, thus, accounting for a nanocrystalline nature. These three phases were found [32] to exist within critical particle size ranges of 50–140 Å, 100–220 Å and 190–420 Å, respectively. On the other hand, the slow kinetics of transformation of metastable zirconia into *m*-ZrO_2 has been ascribed [30] to the reconstructive nature of the process, for *m*-ZrO_2 is distinct amongst the different polymorphs of zirconia of maintaining seven-fold coordinated Zr ions, whereas the others have eight-fold coordinated Zr ions. Therefore, the *c*- to *t*-ZrO_2 transformation has been considered [2] relatively rather facile due to its displacive nature.

SZrOH and PZrOH: Influence of sulphate (SZrOH) and phosphate (PZrOH) additives on the above described polymorphic behavior of zirconia obtained via amorphous ZrOH, is demonstrated by the diffractograms compared in Fig. 3. It is obvious from the results, that the additives hamper the crystallization into metastable zirconia at $\leq$500. This is reflected in the marked weakening of the major peak at 2.959 Å, and the complete suppression of the minor peaks at 2.585 and 2.553 Å, in the diffractograms of both SZrOH(500) and PZrOH(500). The impact of the phosphate additive is relatively more prominent. This also holds for the results exhibited by SZrOH(700) and PZrOH(700). Based on the peak identifications inserted in Fig. 3, one can easily see the hampering influences of the salt additives on the crystallization into metastable zirconia at <700 °C, as well as its eventual transformation into *m*-ZrO_2 at $\geq$700 °C. It is equally noteworthy, that the resolution observed for the two minor peaks in the diffractogram of ZrOH(700) at 2.609 and 2.560 Å is much foorer in

the diffractograms of the corresponding calcination products of SZrOH and PZrOH. As a matter of fact, the former peak is hardly resolved from the latter in the diffractogram of PZrOH(700) (Fig. 3). According to the standard XRD data filed for *c*-ZrO_2 (JCPDS #27–977) and *t*-ZrO_2 (JCPDS #17–923), the peak at 2.609 Å is diagnostic for *t*-ZrO_2, whereas the other (at 2.560 Å) is observed for *c*- or *t*-ZrO_2. Accordingly, one may consider the additives, particularly that of phosphate, to stabilize selectively *c*-ZrO_2, thus, hindering its transformation into *t*-ZrO_2 and, subsequently, *m*-ZrO_2.

Impacts of the salt additives are maintained even after calcination at 1000 °C. Despite the better resolution of the two minor peaks, now at 2.624 and 2.562 Å, in the diffractogram of PZrOH(1000), it is void of any detectable sign of formation of *m*-ZrO_2; namely, the two weak, but distinct, peaks exhibited by ZrOH(1000) at 3.153 and 2.836 Å. They might be observed in the diffractogram of SZrOH(1000) though at still much weaker intensities. Even after a 24 h cooling at RT, the transformation into *m*-ZrO_2 is shown to be retarded in SZrOH(1000), but much more retarded in PZrOH(1000) (Fig. 3). The *m*-ZrO_2 is, in contrast to the case for both ZrOH(1000) and SZrOH(1000), a minor phase in PZrOH(1000). This can be evidenced by the much weaker peaks (at 3.152 and 2.84 Å) of *m*-ZrO_2 than the peak (at 2.959 Å) assignable to *t*- and/or *c*-ZrO_2 in the diffractogram of PZrOH(1000).

It is worth noting, that the predominance of *m*-ZrO_2 after 24 h cooling of ZrOH(1000) is shown to be accompanied not only by predominance of its two diagnostic peaks, but also by reversal of the relative intensities of the two minor peaks, viz. from $I_{2.6}/I_{2.5} < 1$ (after 1 h cooling) to >1 (after 24-cooling). According to the standard XRD data compiled for mononclinic zirconia in ICDD #37–1484, this intensity reversal is consistent with formation of *m*-ZrO_2. The same observation can be made in the diffractogram of the 24 h cooled SZrOH(1000), where the XRD peaks of *m*-ZrO_2 predominate. Therefore, the persistence of the $I_{2.6}/I_{2.5}$ ratio at a value <1, against the prolonged cooling of PZrOH(1000), is another clue for phosphate-induced retardation of the transformation into *m*-ZrO_2.

Summing up, XRD results indicate conversion of the amorphous $Zr(OH)_4$ parent into metastable tetragonal and/or cubic zirconia at 400 °C, which upon further heating are slowly transformed into monoclinic zirconia. Cooling to RT enhances the process; a fact that proves that *m*-ZrO_2 is the thermodynamically stable phase at low temperatures. According to Lajavardi et al. [32], *c*-ZrO_2 crystallizes first from the amorphous parent, and transforms later into *t*-ZrO_2 as its particle size grows larger to exceed ca. 140 Å. On the other hand, the tetragonal zirconia is transformed into *m*-ZrO_2 as its particle size exceeds ca. 220 Å. Thus, these authors [32] ascribe the existence at low temperatures of the otherwise unstable *c*- and *t*-ZrO_2 to their high surface energy. Other investigators [30] preferred, however, to confine the metastability solely to *t*-ZrO_2, and attributed its occurrence to a kinetic retardation, namely, slow transformation of *t*- to *m*-ZrO_2. The presence of sulfate and, particularly, phosphate additives slow further the high-temperature transformation into *m*-ZrO_2. Even after a prolonged cooling at RT, the presence of phosphate suppresses markedly the formation of *m*-ZrO_2. This behaviour might be attributed to an additive-effected stabilization of the precursor metastable phase(s). Although XRD cannot help unambiguously discriminating cubic from tetragonal zirconia, the phosphate-induced ill-resolution of the two minor XRD peaks pointing to d-spacings in the range 2.65–2.50 Å (Fig. 3), and the holding of their relative intensity ($I_{2.6}/I_{2.5}$) below unity, may selectively confine the phosphate-stabilization to *c*-ZrO_2. The fact that the salt additives render the peaks of metastable phases broader may help attributing the additive stabilizing effect to retardation of zirconia particle growth.

3.2. Raman spectra

LRa spectra obtained for ex situ calcination products of ZrOH, SZrOH and PZrOH at 500, 700 and 1000 °C are shown in Fig. 4. A total of eight ill-defined peaks may be discerned in the spectrum of ZrOH(500), five of them occur at frequencies assignable to *t*-ZrO_2 (150, 269, 320, 457 and 640 cm^{-1} [1,34–36]), and the other three occur at frequencies assignable to *m*-ZrO_2 (190, 380 and 557 cm^{-1} [34–36]). Whereas one may recognize two very weak Raman peaks near frequencies assignable to *t*-ZrO_2 (at 266 and 456 cm^{-1}) in the spectrum of SZrOH(500), no peaks whatsoever are detectable in

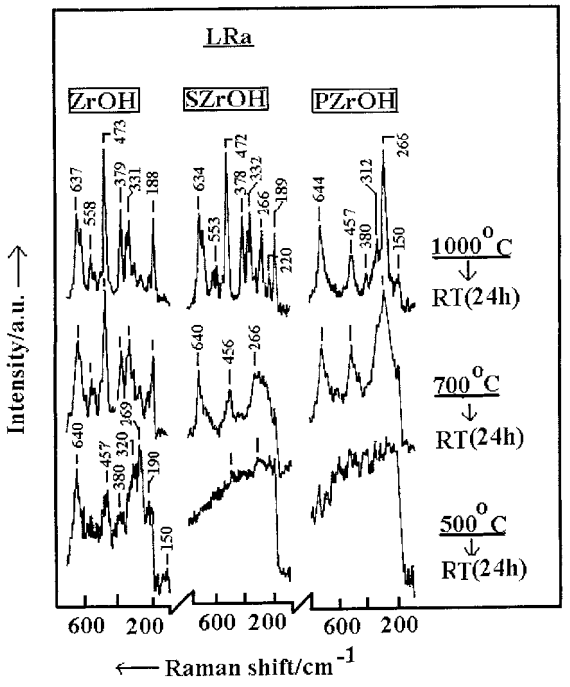

Fig. 4. Infrared spectra taken following cooling at RT for 24 h of ex situ calcined samples of ZrOH, SZrOH and PZrOH at the temperatures indicated for 3 h.

the spectrum exhibited by PZrOH(500). These results are in line with the XRD results (Fig. 3) in accounting for the crystallization retarding influence of the salt additives, particularly of the phosphate.

According to previous Raman studies [34–36], *t*-ZrO_2 has six Ra-active modes, and is diagnosed by peaks at 148 and 263 cm^{-1}. On the other hand, *m*-ZrO_2 has 18 Ra-active modes with diagnostic twin-peaks occurring at 170–180 and 180–190 cm^{-1} [34–36]. Highly symmetric, strain-free *c*-ZrO_2 has a sole Ra-active mode at 480–490 cm^{-1} [36]. It has been reported [34–36], however, that these data are for true (stable) polymorphs of zirconia, and that ion-stabilized *c*-ZrO_2 exhibits several Ra-peaks at frequencies indistinguishable from those of *t*-ZrO_2 due to induced lattice distortions. For instance, Ca-stabilized *c*-ZrO_2 has been found [35] to exhibit six Ra-peaks at 147, 259, 317, 465, 606 and 637 cm^{-1}, which are indeed very close to those often reported for *t*-ZrO_2, viz. 149, 230–240, 267–272, 319, 464, 604–615 and 647 cm^{-1} [34,36]. Even metastable *c*-ZrO_2 has been reported [35] to give rise to more than one Ra-peak. In view of these literature data, one cannot exclude with certainty contribution of *c*-ZrO_2 to peaks assignable to *t*-ZrO_2.

Ra spectra taken of the calcination products of ZrOH at 700 and 1000 °C (Fig. 4) indicate considerable retrogression of the peaks assignable to metastable *t*- and *c*-ZrO_2 with marked development of those indicative of *m*-ZrO_2. In fact, Ra-peaks displayed in the spectrum of ZrOH(1000) occur largely at frequencies assignable to *m*-ZrO_2: 188, 331, 379, 473, 558 and 637 cm^{-1} [34,36]. These peaks are shown to predominate the spectrum of SZrOH(1000), with some minor indications to *t*-ZrO_2 (a diagnostic peak is resolved at 266 cm^{-1}, whereas the other (at 457 cm^{-1}) is most likely shrouded by the *m*-ZrO_2 peak at 472 cm^{-1}). In contrast, SZrOH(700) gives rise to a spectrum predominated by three broad peaks at 266, 456 and 640 cm^{-1}. Similar three peaks are the sole Ra-effects exhibited by PZrOH(700), and are the major peaks observed for PZrOH(1000). The latter material does not show Ra-peaks due to *m*-ZrO_2, but shows instead weak peaks assignable to *t*-ZrO_2 (at 150, 312 and 380 cm^{-1}). Accordingly, one may plausibly suggest assigning the three broad Ra-peaks at 266, 457 and 644 cm^{-1} to contribution from nanocrystallites of *c*-ZrO_2. It is worth reporting, that a set of five bands at 147, 266, 315, 480 and 631 cm^{-1}, i.e. similar to those displayed in the spectrum of PZrOH(1000), were recently measured by Lajavardi et al. [32] for a sample consisting of cubic with low percentage tetragonal zirconia. In that sample, *c*-ZrO_2 existed within a particle size range of 50–140 Å.

Within the above context, the Raman examination results of ex situ calcined ZrOH, SZrOH and PZrOH are consistent with the XRD examination results (Fig. 3) in confirming the metastability of tetragonal and cubic zirconia at low temperatures. They also confirm the stability of monoclininc zirconia at low temperatures. The Raman examination lends a strong support to the XRD-based suggestion of phosphate-stabilization of *c*-ZrO_2, which results in an obvious delay in the transformation of the latter into *m*-ZrO_2, via *t*-ZrO_2, at high temperatures.

3.3. Infrared spectra

Fig. 5 exhibits IR spectra obtained for ex situ calcination products of ZrOH, SZrOH and PZrOH at 400 and 1000 °C. The presentation is confined to

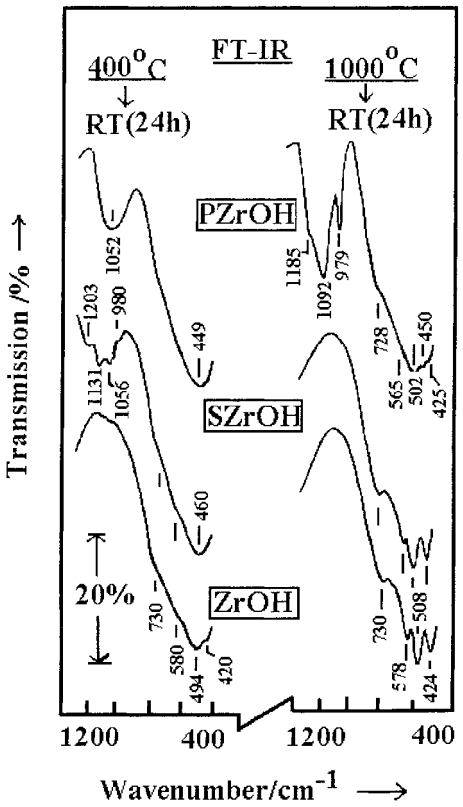

Fig. 5. Laser Raman spectra taken following cooling at RT for 24 h of ex situ calcined samples of ZrOH, SZrOH and PZrOH at the temperatures indicated for 3 h.

the frequency range (1200–400 cm^{-1}) over which S–O, P–O and Zr–O bond vibrations are known to occur [11–13]. The spectra of ZrOH(1000) and SZrOH(1000) are almost identical in displaying nothing, but the diagnostic absorptions of *m*-ZrO_2 at 730(s, sh), 578(vs, sh), 508(vs, sp) and 424(vs, sp) cm^{-1} [13,36]. In contrast, the corresponding 400 °C calcination products give rise to different IR spectral features. Although both ZrOH(400) and SZrOH(400) show similarly a composite, broad absorption (at 950–400 cm^{-1}) due to Zr–O bond vibrations [13,36], each assumes a different fine band structure. Whereas the Zr–O absorption of ZrOH(400) resolves maxima at frequencies (730, 580, 494 and 420 cm^{-1}) corresponding satisfactorily to those of *m*-ZrO_2, the Zr–O absorption of SZrOH(400) resolves instead a sole, strong absorption at 460 cm^{-1}. Another significant difference between the two spectra lies in the display of S–O bond vibrations (at 1203, 1131, 1056 and 980 cm^{-1}) only in the spectrum of SZrOH(400), which are assignable to various modes of S–O bond vibrations of differently structured sulfate species [20]. These results indicate the elimination of sulfate species on calcination at 1000 °C, as has earlier been observed by thermal analysis of a similar SZrOH material [13]. They also indicate that the presence of sulfate at 400 °C retards formation of *m*-ZrO_2. In terms of XRD results of SZrOH(400), one may assign the 460-cm^{-1} absorption to metastable zirconia (i.e. *t*- and/or *c*-ZrO_2).

The spectra taken of PZrOH(400) and (1000) are unique in showing a broad, but rather symmetric, strong absorption at 449 cm^{-1} for the former material, which remains observed (at 450 cm^{-1}) in the spectrum of the latter material. This absorption is very similar to that observed at 448 cm^{-1} for the sole IR-active Zr–O vibration of *c*-ZrO_2 [36]. This is probably the strongest support to the XRD-based suggestion of phosphate-stabilization of cubic, rather than tetragonal zirconia at low temperatures. The other Zr–O absorption maxima resolved in the spectrum of PZrOH(1000) are largely due to coexisting *t*- and *m*-ZrO_2. It is worth noting, that absorptions of P–O vibrations remained stable, but restructured, at 1000 °C. The absorptions resolved in the spectrum of PZrOH(1000) at 1185, 1092 and 979 cm^{-1} have been assigned previously to polymeric phosphate species [19]. Consistently, the corresponding Ra spectrum displayed weak, but distinct, peaks at 1157, 1084 and 1021 cm^{-1}, which have also been considered indicative of pyrophosphate species [11,12]. ZrP_2O_7, the most likely composition of pyrophosphate anchored onto zirconia surfaces, is known to assume a cubic structure [37]. This fact may suggest an additional phosphate-stabilizing element, whereby formation of the pyrophosphate may seed for formation and stabilization of cubic zirconia.

4. Conclusion

The following is an attempt to integrate conclusions that may be drawn from the present results with conclusions drawn previously from relevant investigations carried out by others, into a comprehensive one. Accordingly, amorphous $Zr(OH)_4$ has short-range structures in which the atomic organization is

more analogous to that of cubic (c-ZrO_2) and tetragonal (t-ZrO_2) zirconia than that of the monoclinic (m-ZrO_2) modification [30]. Therefore, heating of the hydroxide at 400 °C leads to dehydration and incipient crystallization of zirconia thus genesized into a mixture of metastable phases of c- and t-ZrO_2, which is rendered richer in the cubic phase the smaller the particle size [30,32]. Upon increasing the temperature up to 1000 °C, a slow transformation of c- into t-ZrO_2 and, subsequently, m-ZrO_2, takes place in response to particle growth [30,32]. The transformation into m-ZrO_2 is speeded up considerably following subsequent cooling to room temperature. Thus, the monoclinic modification is proven to be the low-temperature stable (true) phase of zirconia.

Sulfate and phosphate additives retard the transformation into m-ZrO_2, an effect that is much more obvious with the phosphate additive. Reasons for that may be two-fold. It may be either that these additives suppress particle sintering (growth), or that they stabilize both, or either of the metatstable polymorphs (t- and/or c-ZrO_2). It is tempting to suggest phosphate additives to stabilize preferentially c-ZrO_2. The thrust behind this suggestion is the fact that phosphate additives form cubic zirconium pyrophosphate species (ZrP_2O_7) that could then seed for the crystallization of the decomposition product of the hydroxide into cubic zirconia. This suggestion is not entirely groundless, for it may find a reasonable support by the present results, particularly the Raman and infrared spectroscopic results.

Acknowledgements

We acknowledge with appreciation the analytical support of SAF general facility projects funded by Kuwait University Research Administration, and the zirconium hydroxide donation of MEL, UK.

References

[1] V.G. Keramidas, W.B. White, J. Am. Ceram. Soc. 57 (1974) 22.
[2] D.K. Smith, H. Newkirk, Acta Cryst. 18 (1965) 983.
[3] Y. Amenomiya, Appl. Catal. 30 (1987) 57.
[4] T. Iizuka, M. Koijma, K. Tanabe, J. Chem. Soc., Chem. Commun. 1983, p. 638.
[5] L.A. Bruce, G.J. Hope, J.F. Mathews, Appl. Catal. 8 (1983) 349.
[6] R.A. Dalla Betta, A.G. Piken, M. Shelef, J. Catal. 40 (1975) 173.
[7] T. Yamaguchi, Appl. Catal. 61 (1990) 1.
[8] K. Arata, Adv. Catal. 37 (1990) 165.
[9] G. Ertl, H. Knözinger, J. Weitkamp (Eds.), Handbook of Heterogeneous Catalysis, Vol. 1, Wiley-VCH, Weinheim, 1997, pp. 118–412.
[10] G.A.H. Mekhemer, H.M. Ismail, Coll. Surf. A 164 (2000) 227.
[11] M.I. Zaki, A.A.M. Ali, Coll. Surf. 119 (1996) 39.
[12] A.A.M. Ali, M.I. Zaki, Coll. Surf. 139 (1998) 81.
[13] A.A.M. Ali, M.I. Zaki, Thermochim. Acta 336 (1999) 17.
[14] K. Tanabe, H. Hattori, in: G. Ertl, H. Knözinger, J. Weitkamp (Eds.), Handbook of Heterogeneous Catalysis, Vol. 1, Wiley-VCH, Weinheim, 1977, pp. 404–412.
[15] M. Waqif, J. Bchelier, O. Sauer, J.C. Lavalley, J. Mol. Catal. 72 (1992) 127.
[16] A. Corma, A. Martinez, C. Martinez, J. Catal. 149 (1994) 52.
[17] T. Riemer, D. Spielbauer, M. Hunger, G.A.H. Mekhemer, H. Knözinger, J. Chem. Soc., Chem. Comm. 1994, p. 1181.
[18] D. Spielbauer, G.A.H. Mekhemer, T. Riemer, M.I. Zaki, H. Knözinger, J. Phys. Chem. 101 (1997) 4681.
[19] G. Busca, V. Lorenzelli, P. Galli, A. Ginestra, P. Patrono, J. Chem. Soc., Faraday Trans. I 83 (1987) 853.
[20] E. Steger, W. Schmidt, Ber. Bunsenges. Phys. Chem. 68 (1964) 102.
[21] P. Duwez, F. Odell, J. Am. Ceram. Soc. 33 (1950) 274.
[22] P. Duwez, F. Odell, F.H. Brown Jr., J. Am. Ceram. Soc. 35 (1952) 107.
[23] C.H. Perry, D.W. Liu, J. Am. Ceram. Soc. 68 (1985) 184.
[24] R.M. Potter, G.R. Rossman, Am. Min. 64 (1979) 1199.
[25] K. Khadzhiivanov, A. Davydov, Kinetic Katal. 29 (1988) 460.
[26] A. Dicko, X. Song, A. Adnot, A. Sayari, J. Catal. 150 (1994) 254.
[27] J.M. Parera, Catal. Today 15 (1992) 481.
[28] M. Yamasaki, H. Habazaki, T. Yoshida, E. Akiyama, A. Kawashima, K. Asami, K. Hashimoto, M. Komori, K. Shimamura, Appl. Catal. A 163 (1997) 187.
[29] H. Habazaki, T. Yoshida, M. Yamasaki, M. Komori, K. Shimamura, E. Akiyama, A. Kawashima, K. Hashimoto, in: T. Inui, et al. (Eds.), Advances in Chemical Conversions for Mitigating Carbon Dioxide, Studies in Surface Science and Catalysis, Vol. 114, Elsevier, Amsterdam, 1998, pp. 261–266.
[30] P.D.L. Mercera, J.G. Van Ommen, E.B.M. Doesburg, A.J. Burggraaf, J.R.H. Ross, Appl. Catal. 57 (1990) 127.
[31] S. Ardizzone, C.L. Bianchi, E. Grassi, Coll. Surf. 135 (1998) 41.
[32] M. Lajavardi, D.J. Kenney, S.H. Lin, J. Chinese Chem. Soc. 47 (2000) 1043, 1055 and 1065.
[33] W.K. Hall, Proc. Phys. Soc. London, Ser. A 62 (1972) 1838.
[34] M. Ishigame, T. Sakurai, J. Am. Ceram. Soc. 60 (1977) 367.
[35] D.P.C. Thackeray, Spectrochim. Acta 30A (1974) 549.
[36] C.M. Philippi, K.S. Mazdiyasni, J. Am. Ceram. Soc. 54 (1971) 254.
[37] E. Steger, G. Leukroth, Z. Anorg. Allg. Chem. 303 (1960) 169.